Environmental Science Nano

Rapid Organic Solvent Extraction Coupled with Surface Enhanced Raman Spectroscopic Mapping for Ultrasensitive Quantification of Foliarly Applied Silver Nanoparticles in Plant Leaves

Journal:	*Environmental Science: Nano*
Manuscript ID	EN-COM-11-2019-001246.R1
Article Type:	Communication

Environmental Significance

One consistent challenge in studying the behavior and impact of silver nanoparticles (AgNPs) in crop plants is how to detect and quantify them. The present study developed a rapid (2h) organic solvent extraction method to extract AgNPs from plant tissues. The morphology of extracted AgNPs were greatly preserved during the extraction process, which is an advantage over both alkaline and enzymatic digestion methods. Followed by filtration and surface enhanced Raman spectroscopic (SERS) mapping, we successfully detected and quantified the extracted AgNPs within 15 min. This research highlights the superior potential of the organic solvent method coupled with SERS mapping to study the fate and behavior of AgNPs in plant tissues.

Rapid Organic Solvent Extraction Coupled with Surface Enhanced Raman Spectroscopic Mapping for Ultrasensitive Quantification of Foliarly Applied Silver Nanoparticles in Plant Leaves

Zhiyun Zhang[1], Ming Xia[1,2], Chuanxin Ma[3], Huiyuan Guo[4], Wenhao Wu[4], Jason C. White[3], Baoshan Xing[4], and Lili He[1]

[1]Department of Food Science, University of Massachusetts, Amherst, Massachusetts 01003, United States

[2]College of Pharmacy, Zhejiang Chinese Medical University, Zhejiang Province 310053, P. R. China

[3]Department of Analytical Chemistry, The Connecticut Agricultural Experiment Station, New Haven, Connecticut 06511, United States

[4]Stockbridge School of Agriculture, University of Massachusetts, Amherst, Massachusetts 01003, United States

*** Corresponding Author:** Lili He,
Mailing Address: 240 Chenoweth Laboratory, 102 Holdsworth Way, Amherst, MA 01003,
E-mail: lilihe@foodsci.umass.edu,
Telephone: +1 (413) 545-5847

ABSTRACT

A rapid (2h) organic solvent-based approach was developed to extract silver nanoparticles (AgNPs) from spinach leaves. The extracted AgNPs were enriched on a filter membrane and quantified by a surface enhanced Raman spectroscopic (SERS) mapping technique. The lowest detectable concentration of AgNPs was 1 ng/mL and the accuracy was 74-113%.

Due to their excellent physical and antimicrobial properties, silver nanoparticles (AgNPs) are one of the most commonly used engineered nanomaterials globally.[1] It is inevitable that AgNPs are intentionally or unintentionally released to the environment with this increasing usage, posing potential negative impacts on environmental and human health.[2–8] Thus, understanding the biological fate of AgNPs is important to be able to accurately assess the risk they pose. However, considering the extremely low concentration of AgNPs in numerous environmental matrices, as well as their chemical and physical instability, being able to sensitively, reliably and cost-effectively detect and quantify AgNPs remains as a significant challenge.[9,10]

Currently, synchrotron X-ray absorption near-edge spectroscopy (XANES) and single particle inductively coupled plasma mass spectrometry (sp-ICP-MS) are the most widely used techniques for engineered nanoparticle (ENPs) detection and quantification in different environmental matrices.[11–15] However, XANES requires complex sample preparation and is only used for qualitative analysis. sp-ICP-MS can provide both qualitative and quantitative results of AgNPs with sizes larger than 20 nm but this technique is limited by the capability of the instrument to distinguish nanoparticle pulse signals from background noise.[16] Also, it is impossible to apply these techniques for routine AgNPs analysis due to their limited accessibility and high requirements for well-trained operators.[17] Surface enhanced Raman spectroscopy (SERS) has recently become an alternative option and several studies regarding SERS use to detect and quantify AgNPs in consumer products, environmental surface water and plant extracts have been reported.[15,18–22] Given the specific interactions between AgNPs and indicator molecules and the resulting strong SERS enhancement, AgNPs can readily be

differentiated from other Ag species. In addition, detection is possible at extremely low concentrations of AgNPs at a size range from 5 to 200 nm in aqueous samples.[15,19–21,23] However, even the lowest limit of detection (LOD) of AgNPs in these reported studies is still higher than common predictions of AgNPs (~80 ng/L) in the environment. In addition, matrix interferences, especially strong fluorescent interferences, were reported to negatively interfere with SERS signals.[15,22] Furthermore, all of the previous studies were focused on liquid matrices, which limits the applicability of SERS-based protocols to detect AgNPs in solid matrices such as plant tissues. As such, this approach has not been an effective tool to comprehensively study the biological fate of AgNPs in crop plants.

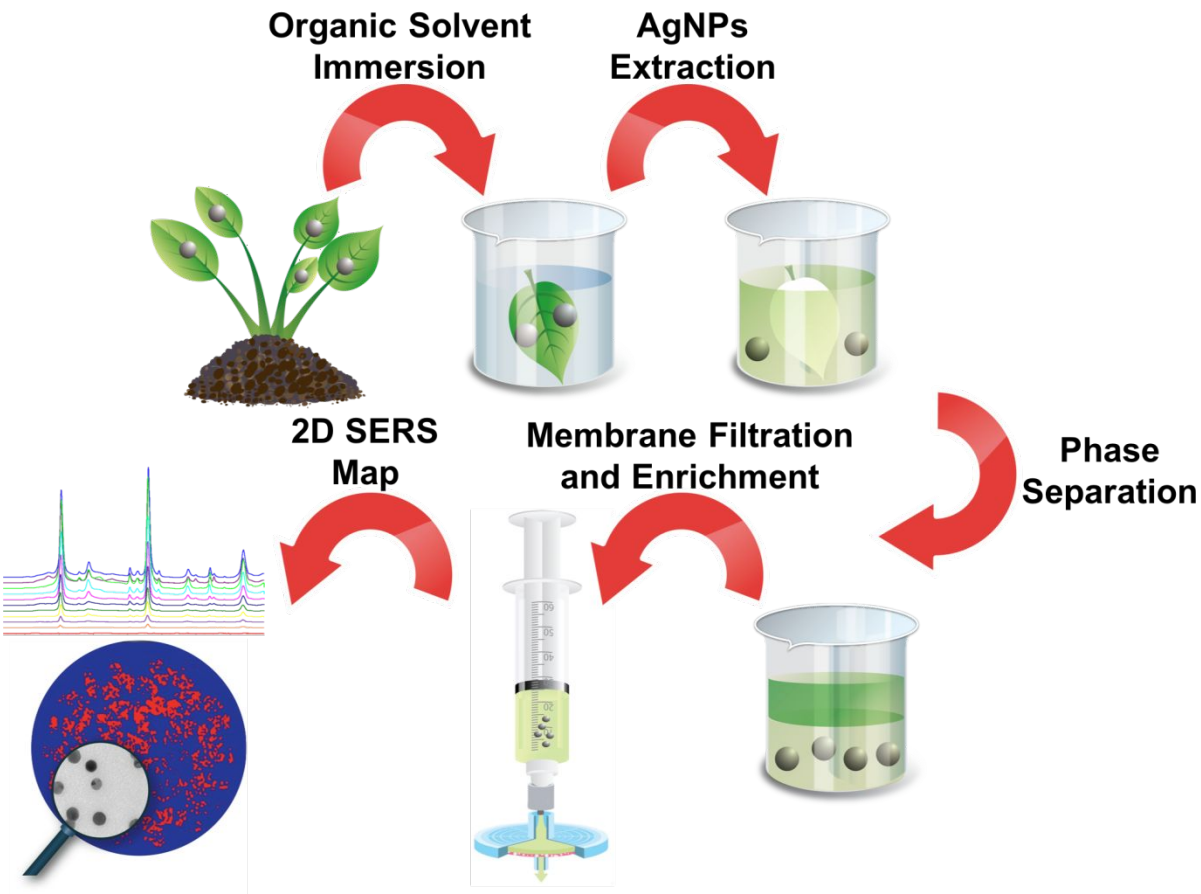

Fig. 1 Schematic diagram illustrating the procedure to detect and quantify AgNPs by organic solvent-based AgNPs extraction coupled with a SERS mapping technique.

In this study, we developed a rapid organic solvent-based method to extract foliar applied AgNPs from spinach leaves. To the best of our knowledge, this is the first time that organic solvents instead of acids, alkalines or enzymes were used to extract AgNPs from plant tissue. We also improved SERS sensitivity by reducing fluorescent interferences and concentrating the extracted AgNPs on a filter membrane. A SERS mapping technique was used to scan the membrane for quantitative analysis.

The idea of using an organic solvent to extract AgNPs from spinach leaves was inspired from the protocol for pigment extraction, where organic solvents are used to extract chlorophylls and carotenoids from plant tissues.[24] In addition, Myung et al. showed the epicuticular wax layer of plant leaves could be altered by organic solvent solutions.[25] To evaluate this protocol when combining with the 4-Mercaptobenzoic acid (4-MBA) labelling strategy we previously developed,[15] we used 60 nm citrate coated AgNPs (CIT-AgNPs, 20 $\mathrm{ng/\mu L}$, Nanocomposix, CA) and spinach leaves as the model system. Briefly, four $\mu\mathrm{L}$ of 60 nm CIT-AgNPs were pipetted onto a section of freshly harvested spinach leaf (0.5 g) and dried in the fume hood. After drying, this portion of leaf was completely immersed into a 1000 $\mu\mathrm{g/mL}$ 4-Mercaptobenzoic acid (4-MBA) solution amended with acetone (8 mL) and methanol (2 mL) on a nutating mixers (Fisher Scientific, Hampton, NH) for 2 h. The wax layer (e.g. 1-octacosanol) of the spinach leaf was immediately dissolved by the methanol and acetone.[25] Subsequently, AgNPs in the spinach leaves were surface labelled by attachment of the 4-MBA molecules in the organic solvent due to the high affinity of the 4-MBA thiol group to

AgNPs.[12] Importantly, 4-MBA labelled AgNPs are hydrophobic due to the presence of a benzene ring and carboxylic group, which facilitates the extraction of AgNPs with the aid of the organic solvents. After 2 h, the spinach leaf totally turned white in color since AgNPs and the carotenes/chlorophylls were extracted from the tissue (**Fig. 2A**). The AgNPs extraction efficiency was determined by inductively coupled plasma mass spectrometry (ICP-MS) (ICP-MS 2030, Shimadzu); the results showed that 57 $\pm$ 2% of the total AgNPs could be successfully extracted. The detailed protocol for ICP-MS determination is provided in the supporting information. The extraction efficiency of foliarly applied AgNPs from spinach leaves is mainly determined by four factors, 1) the position of the AgNPs after foliar application. Based on our previous study, most of the foliar applied AgNPs were remained on the surface and can be removed by a sodium hypochlorite and ammonium hydroxide combined washing method.[26] 2) the efficacy of the organic solvent to remove epicuticular wax layer, 3) the binding capability of 4-MBA with the AgNPs, and 4) the transformation of AgNPs after foliar application. It should be noteworthy to mention that, some of AgNPs may transform to other SERS inactive silver species after foliar exposure, including Ag^+ species, AgCl-NPs, Ag_2S and Ag-glutathione.[27]

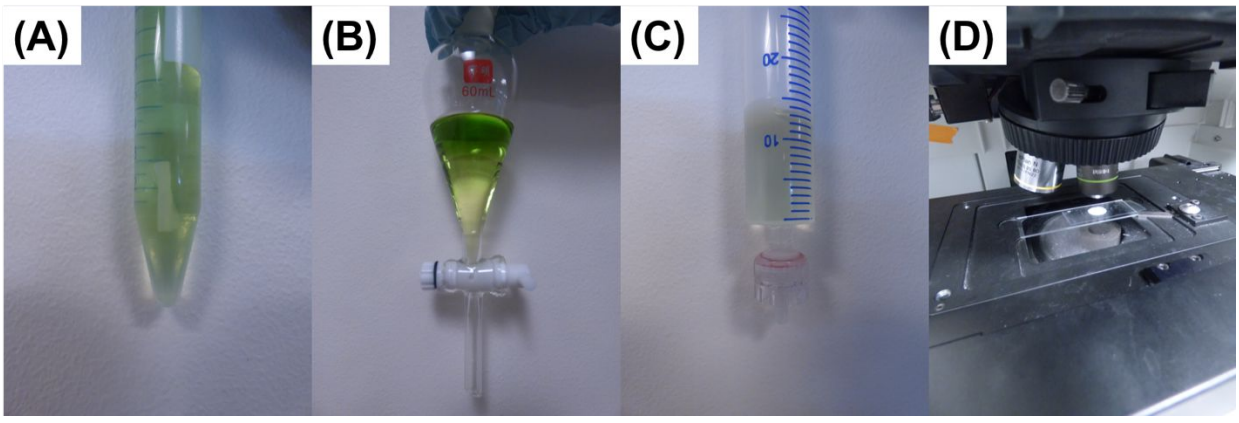

Fig. 2 (A). 60 nm CIT-AgNPs contaminated spinach leaves were immersed in 1000 mg/L 4-MBA organic solvent solution (2 mL methanol and 8 mL acetone); (B). 10 mL DI water and acetyl acetate were mixed with the original organic solution and separated by phase; (C) The lower phase in (B) was filtered through PTFE membrane with pore sizes of 0.2 μm; (D) Raman Detection and Analysis.

Previous studies with AgNPs detection in plant tissues showed significant fluorescence interference.[15] In this study, we further developed a protocol to separate extracted AgNPs from the plant pigments by transforming the hydrophobic AgNPs to be hydrophilic and then extract the particles in the water phase, leaving the pigments in the organic phase. Specifically, DI water and ethyl acetate were added into methanol/acetone solution at an equal volume ratio and the pH of the resulting solution was adjusted by sodium hydroxide (wt. 40%) to ≥ 9.0. After pH adjustment, all the surface attached 4-MBA molecules (pKa (carboxylic head) ~ 7.4) were fully deprotonated, which rendered AgNPs to be hydrophilic and forced the particles into the bottom layer of the solution. ICP-MS analysis showed that 87 ± 2% of the total AgNPs were detected in this layer. After that, the bottom layer was filtered through a 0. 22 μm polytetrafluoroethylene (PTFE) filter membrane (EMD Millipore, Burlington, MA) using a syringe. This filter membrane was then dried and analyzed using DXRxi Raman spectroscopy (Thermo Scientific, Madison, WI). Considering the diameter (13 mm) of the PTFE filter membrane, a 13 mm × 13 mm square mapping area was constructed based on the Raman peak of 4-MBA at 1078 cm^{-1}. Since minimized scanning time is preferable in this study, a short spectral acquisition time (0.05s for each spectrum) and the largest allowable step size setting (100 μm) were adopted, which ensures the scanning time of each map to be limited within 15 min. It is noted that small AgNPs aggregates on the filter membrane may not be detected due to this comparative large

step size. Thus, in a future study, a compromise between scanning time and step size will be investigated. To analyze the image, 1000 cps was set as the cut-off intensity to determine the presence of AgNPs on the SERS map, where red color indicates the presence of AgNPs and blue represents particle absence (**Fig. 3B**). The cut-off line was set based on the intensity of the filter membrane background ($S_{cut\ off} = S_{blank} + 3\sigma_{blank}$), where S_{blank} is the signal intensity of peak at 1078 cm^{-1} for a blank membrane, and σ_{blank} is the known standard deviation for the blank membrane's signal. **Fig. 3C** is the representative SERS spectrum extracted from SERS image. Four characteristic peaks of 4-MBA at 1588, 1178, 1130, and 1076 cm^{-1} were observed and they are attributed to the ν (C−C) ring stretching, δ (C−H) deformation modes, δ (C−H) deformation modes, and ν (C−C) ring breathing, respectively.[28] Compared with our previous study,[15] little background noise was observed within the Raman shift between 1200 to 400 cm^{-1}, indicating the fluorescent interference was largely eliminated. Also, it is noted that the average size of extracted AgNPs were non-statistically different from the size of original particles (**Fig. 4**), indicating our method retains the morphology of AgNPs during the extraction process. This is an advantage over both alkaline and enzyme digestion methods which need approximately 24-36 h at relatively high (alkaline) or low (enzyme) pH to function and likely change AgNPs morphology during the extraction process.[13,14] The SEM image also shows the aggregation status of the AgNPs after extraction. The aggregation status is important for both membrane filtering efficiency and SERS activity. After aggregation, the AgNP aggregates can be efficiently retained on the 0.22 μm filter membrane which can also be visually observed at higher concentrations. The

aggregation also provides sufficient hot spots for SERS activity, thus facilitating the high sensitivity of this approach.

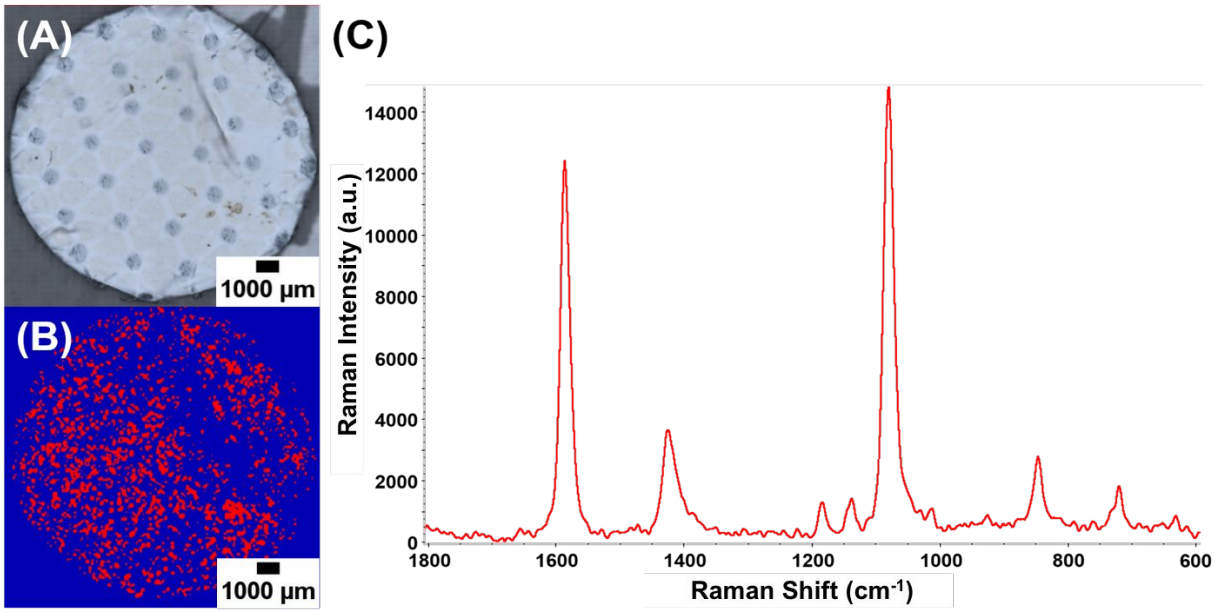

Fig. 3 60 nm CIT-AgNPs (80 ng) extracted from a spinach leaf (0.5 g). Optical Image (A), Raman scattering image (B) and average SERS spectrum (C) of extracted AgNPs on the filter membrane. The unit of a.u. is the abbreviation of arbitrary unit.

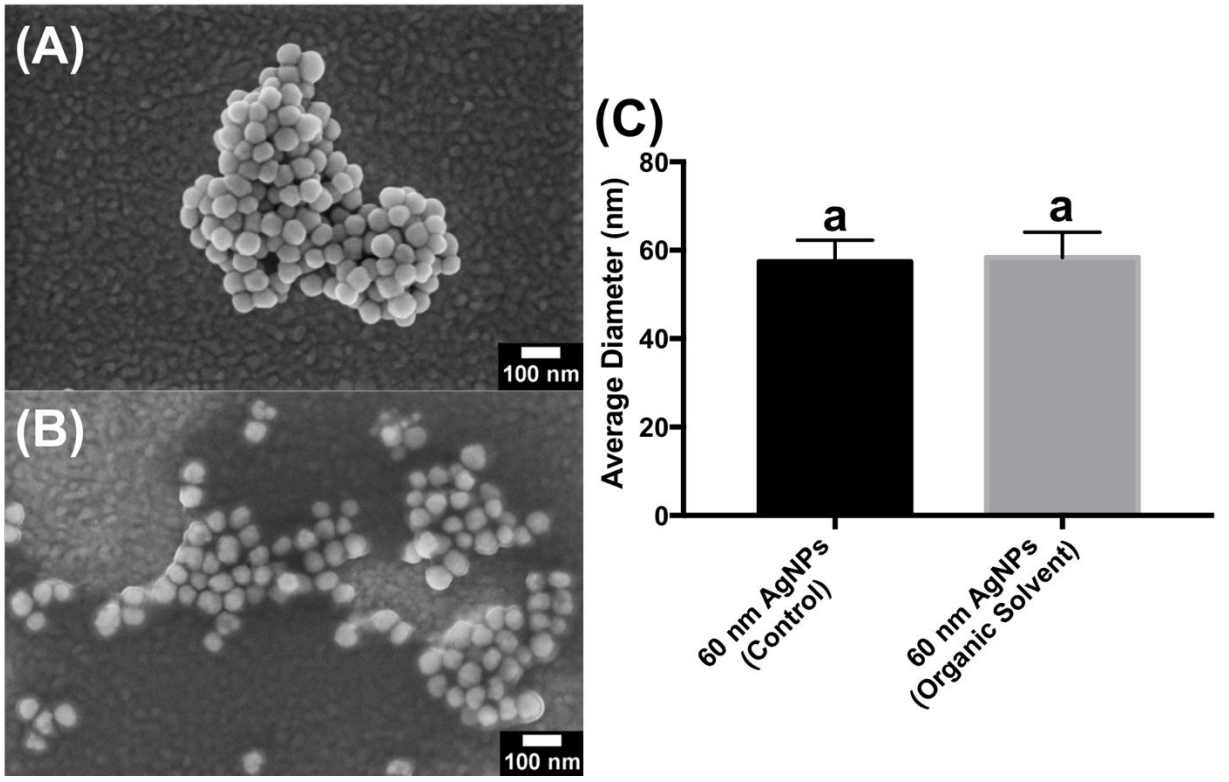

Fig. 4 SEM image of 60 nm CIT-AgNPs Control (A); 60 nm CIT-AgNPs extracted from spinach leaf by organic solvent (B); Size distribution analysis.

In addition, the feasibility of using SERS mapping to quantify the extracted AgNPs was further investigated by testing the 60 nm CIT AgNPs over a concentration range of 0-8 ng/mL. As evident in **Fig. 5**, the amounts of red spots in the SERS map was positively correlated with the AgNPs amounts in the tested range. As such, we tried to quantify the amount of loaded AgNPs on the filter membrane by three different methods. The first two methods were based on the average intensity of selected spectra and the only difference between them are the amounts of spectra. In the first method, the spectra from 10 random red spots were averaged. We only selected 10 random spots for analysis due to the fact that at lower concentrations, only a small number few red spots were observed. Thus, to maintain consistency, only 10 random spots were

selected from the red areas in each map. In the second method, all the spectra from the whole map were averaged by a built-in function of the OMNICxi software (Thermo Scientific). The third method is based on counting the total pixel area of red spots in the image, which could also be achieved using the built-in function of the software, or a free imaging analysis tool named ImageJ.[29] As shown in **Fig. 5**, we found all these three methods show the positive trends when increasing the amounts of AgNPs loaded on the filter membrane in the function of polynomial and with reasonable linearity between 1~8 ng/mL, indicating all these three methods could be used within AgNPs in this concentration range. It should be noted that although the lowest detectable concentration of AgNPs in this experiment is 1 ng/mL, lower detection limits could be achieved by increasing the sample volume. In addition, the accuracy of these three quantitative methods were evaluated based on the following equation,

$$\%\mathrm{RV} = \left(\frac{[AgNPs]_{calculated}}{[AgNPs]_{nominal} \times \eta_P \times \eta_S}\right) \times 100$$

where η_P and η_S refer to the extraction efficiency of AgNPs from plants and the organic solvent system, which was determined to be 57% and 87%, respectively. The nominal concentration of AgNPs translated from 80 ng in 0.5 g spinach leaf sample to aqueous sample was 8 ng/mL.

As shown in Table 1, we found it is more accurate to quantify the amount of extracted AgNPs based on either the average Raman intensity from 10 random spectra (**Method 1**) or the total pixel area of red spots in the image (**Method 3**). It is important to mention that using **Method 3** for AgNPs quantitation would be preferable since the

number of pixels is independent of the peak intensity, as long as the intensity is above the cut-off line. This method may be potentially applied to different sizes or aggregation state of AgNPs and we will evaluate this hypothesis in the future study. Comparing **Method 1 and 2**, **Method 2** yielded much less intensity as the majority of the maps are in blue color, resulting in less sensitivity for AgNPs detection. Both **Method 1 and 2** are highly dependent on the size and aggregation state of the AgNPs.

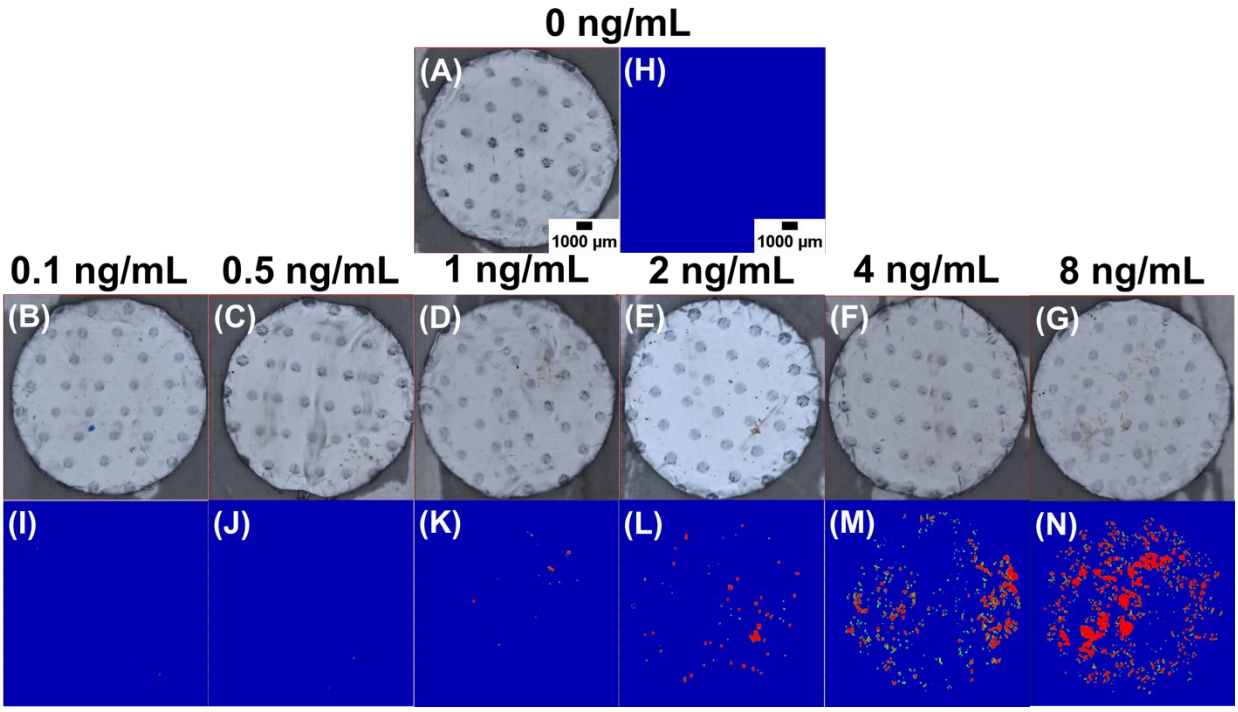

Fig. 5 Different amount of 60 nm CIT-AgNPs on the filter membrane. Optical images: (A)-(C), (G)-(I); Raman scattering images: (D)-(F), (J)-(L). Laser wavelength=780 nm, Laser intensity=5 mW, aperture= 50 slit, step size= 100 µm, scan rate=0.05 s/step.

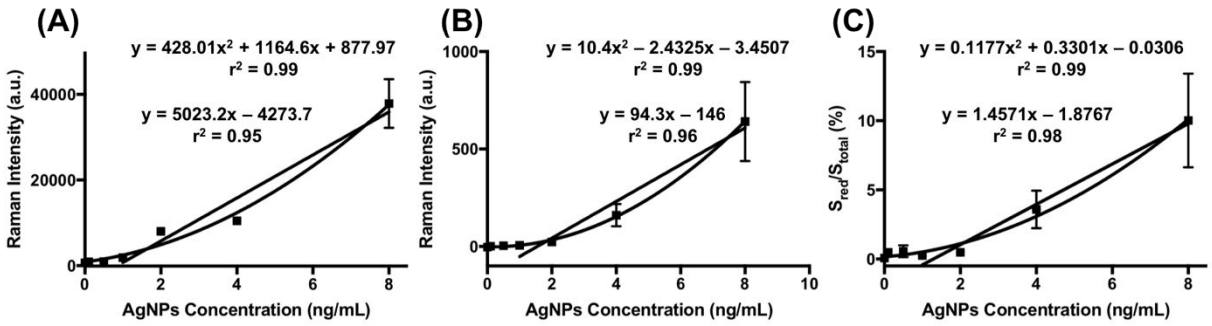

Fig. 6 Concentration-dependent SERS response to AgNPs, (A). 10 spectra average (B). whole map average, (C). The percentage of area occupied by AgNPs in SERS map. The error bars represent the standard errors of three parallel SERS measurements.

Table 1. Comparison of different methods to quantify AgNPs on the filter membrane.

	Method 1	Method 2	Method 3
Correlation Coefficient (1~8 ng/mL)	**0.95**	**0.96**	**0.98**
SERS Intensity	**14803 (a.u.)**	**130 (a.u.)**	**4.7 (%)**
Corresponding Concentration of AgNPs	**3.8 (ng/mL)**	**2.9 (ng/mL)**	**4.5 (ng/mL)**
Accuracy	**96%**	**74%**	**113%**

In conclusion, a simple and rapid organic solvent-based extraction method coupled with SERS mapping to quantify the amounts of AgNPs in plant leaves has been developed. Compared with traditional alkaline (tetramethylammonium hydroxide, TMAH) and enzymatic (Macerozyme R-10) digestion methods, the organic solvent-based method needs less time to extract AgNPs (2 h) from plant leaves and importantly, the morphology and size of the AgNPs is largely preserved. Also, compared with sp-ICP-MS, complex and tedious sample preparations are avoided and the amounts of AgNPs could be rapidly quantified using the SERS mapping, which takes only 15 min for

scanning one filter membrane. This study demonstrates the superior potential of this method as a screening tool to study the fate and behavior of AgNPs in plant tissues. In our future work, we will evaluate this method with other types and sizes of AgNPs and sample matrices.

Conflict of Interest

There are no conflicts of interest to declare.

Acknowledgements

We acknowledge USDA-NIFA 2015-67017-23070 for funding this project.

REFERENCES

1 B. Nowack, H. F. Krug and M. Height, 120 years of nanosilver history: implications for policy makers, *Environ. Sci. Technol.*, 2011, **45**, 1177–1183.

2 C. M. Rico, S. Majumdar, M. Duarte-Gardea, J. R. Peralta-Videa and J. L. Gardea-Torresdey, Interaction of nanoparticles with edible plants and their possible implications in the food chain, *J. Agric. Food Chem.*, 2011, **59**, 3485–3498.

3 Y. Deng, J. C. White and B. Xing, Interactions between engineered nanomaterials and agricultural crops: implications for food safety, *J. Zhejiang Univ. Sci. A*, 2014, **15**, 552–572.

4 J. D. Judy, J. M. Unrine and P. M. Bertsch, Evidence for biomagnification of gold

nanoparticles within a terrestrial food chain, *Environ. Sci. Technol.*, 2011, **45**, 776–781.

5 J. D. Judy, J. M. Unrine, W. Rao and P. M. Bertsch, Bioavailability of gold nanometerials to plants: importance of particle size and surface coating, *Environ. Sci. Technol.*, 2012, **46**, 8467–8474.

6 J. L. Gardea-Torresdey, C. M. Rico and J. C. White, Trophic transfer, transformation, and impact of engineered nanomaterials in terrestrial environments, *Environ. Sci. Technol.*, 2014, **48**, 2526–2540.

7 P. V AshaRani, G. Low Kah Mun, M. P. Hande and S. Valiyaveettil, Cytotoxicity and genotoxicity of silver nanoparticles in human cells, *ACS Nano*, 2009, **3**, 279–290.

8 S. Kim, J. E. Choi, J. Choi, K.-H. Chung, K. Park, J. Yi and D.-Y. Ryu, Oxidative stress-dependent toxicity of silver nanoparticles in human hepatoma cells, *Toxicol. In Vitro*, 2009, **23**, 1076–1084.

9 L. Li, K. Leopold and M. Schuster, Effective and selective extraction of noble metal nanoparticles from environmental water through a noncovalent reversible reaction on an ionic exchange resin, *Chem. Commun.*, 2012, **48**, 9165-9167.

10 C. Levard, E. M. Hotze, G. V. Lowry and G. E. Brown, Environmental transformations of silver nanparticles: impact on stability and toxicity, *Environ. Sci. Technol.*, 2012, **46**, 6900–6914.

11 J. A. Hernandez-Viezcas, H. Castillo-Michel, J. C. Andrews, M. Cotte, C. Rico, J. R. Peralta-Videa, Y. Ge, J. H. Priester, P. A. Holden and J. L. Gardea-Torresdey, In situ synchrotron X-ray fluorescence mapping and speciation of CeO2 and ZnO

nanoparticles in soil cultivated soybean (Glycine max), *ACS Nano*, 2013, **7**, 1415–1423.

12 C. Larue, H. Castillo-Michel, S. Sobanska, L. Cécillon, S. Bureau, V. Barthès, L. Ouerdane, M. Carrière and G. Sarret, Foliar exposure of the crop Lactuca sativa to silver nanoparticles: evidence for internalization and changes in Ag speciation, *J. Hazard. Mater.*, 2014, **264**, 98–106.

13 D. Bao, Z. G. Oh and Z. Chen, Characterization of silver nanoparticles internalized by Arabidopsis plants using single particle ICP-MS analysis, *Front. Plant Sci.*, 2016, **7**, 32.

14 Y. Dan, W. Zhang, R. Xue, X. Ma, C. Stephan and H. Shi, Characterization of gold nanoparticle uptake by tomato plants using enzymatic extraction followed by single-particle inductively coupled plasma-mass spectrometry analysis, *Environ. Sci. Technol.*, 2015, **49**, 3007–3014.

15 H. Guo, B. Xing, J. White, A. Mukherjee and L. He, Ultra-sensitive determination of silver nanoparticles by surface-enhanced Raman spectroscopy (SERS) after hydrophobization-mediated extraction, *Analyst*, 2016, **141**, 5261–5264.

16 S. Lee, X. Bi, R. B. Reed, J. F. Ranville, P. Herckes and P. Westerhoff, Nanoparticle size detection limits by single particle ICP-MS for 40 elements, *Environ. Sci. Technol.*, 2014, **48**, 10291–10300.

17 H. Guo, L. He and B. Xing, Applications of surface-enhanced Raman spectroscopy in the analysis of nanoparticles in the environment, *Environ. Sci. Nano*, 2017, **4**, 2093–2107.

18 Z. Zhang, H. Guo, Y. Deng, B. Xing and L. He, Mapping gold nanoparticles on

and in edible leaves in situ using surface enhanced Raman spectroscopy, *RSC Adv.*, 2016, **6**, 60152–60159.

19 H. Guo, Z. Zhang, B. Xing, A. Mukherjee, C. Musante, J. C. White and L. He, Analysis of silver nanoparticles in antimicrobial products using surface-enhanced Raman spectroscopy (SERS), *Environ. Sci. Technol.*, 2015, **49**, 4317–4324.

20 H. Guo, B. Xing and L. He, Development of a filter-based method for detecting silver nanoparticles and their heteroaggregation in aqueous environments by surface-enhanced Raman spectroscopy, *Environ. Pollut.*, 2016, **211**, 198–205.

21 H. Guo, B. Xing, L. C. Hamlet, A. Chica and L. He, Surface-enhanced Raman scattering detection of silver nanoparticles in environmental and biological samples, *Sci. Total Environ.*, 2016, **554**–**555**, 246–252.

22 T. H. D. Nguyen, P. Zhou, A. Mustapha and M. Lin, Use of aminothiophenol as an indicator for the analysis of silver nanoparticles in consumer products by surface-enhanced Raman spectroscopy, *Analyst*, 2016, **141**, 5382–5389.

23 H. Guo, L. C. Hamlet, L. He and B. Xing, A field-deployable surface-enhanced Raman scattering (SERS) method for sensitive analysis of silver nanoparticles in environmental waters, *Sci. Total Environ.*, 2019, **653**, 1034–1041.

24 H. K. Lichtenthaler and C. Buschmann, Extraction of phtosynthetic tissues: chlorophylls and carotenoids, *Curr. Protoc. food Anal. Chem.*, 2001, **1**, F4-2.

25 K. Myung, A. P. Parobek, J. A. Godbey, A. J. Bowling and H. E. Pence, Interaction of organic solvents with the epicuticular wax layer of wheat leaves, *J. Agric. Food Chem.*, 2013, **61**, 8737–8742.

26 Z. Zhang, H. Guo, C. Ma, M. Xia, J. C. White, B. Xing and L. He, Rapid and

efficient removal of silver nanoparticles from plant surfaces using sodium hypochlorite and ammonium hydroxide solution, *Food Control*, 2019, **98**, 699–709.

27 C. C. Li, F. Dang, M. Li, M. Zhu, H. Zhong, H. Hintelmann and D. M. Zhou, Effects of exposure pathways on the accumulation and phytotoxicity of silver nanoparticles in soybean and rice, *Nanotoxicology*, 2017, **11**, 699–709.

28 Z. Zhang, H. Guo, T. Carlisle, A. Mukherjee, A. Kinchla, J. C. White, B. Xing and L. He, Evaluation of Postharvest Washing on Removal of Silver Nanoparticles (AgNPs) from Spinach Leaves, *J. Agric. Food Chem.*, 2016, **64**, 6916–6922.

29 C. A. Schneider, W. S. Rasband and K. W. Eliceiri, NIH Image to ImageJ: 25 years of image analysis, *Nat. Methods*, 2012, **9**, 671.

SUPPORTING INFORMATION

Rapid Organic Solvent Extraction Coupled with Surface Enhanced Raman Spectroscopic Mapping for Ultrasensitive Quantification of Foliarly Applied Silver Nanoparticles in Plant Leaves

Zhiyun Zhang[1], Ming Xia[1,2], Chuanxin Ma[3], Huiyuan Guo[4], Wenhao Wu[4], Jason C. White[3], Baoshan Xing[4], and Lili He[1]

[1]Department of Food Science, University of Massachusetts, Amherst, Massachusetts 01003, United States

[2]College of Pharmacy, Zhejiang Chinese Medical University, Zhejiang Province 310053, P. R. China

[3]Department of Analytical Chemistry, The Connecticut Agricultural Experiment Station, New Haven, Connecticut 06511, United States

[4]Stockbridge School of Agriculture, University of Massachusetts, Amherst, Massachusetts 01003, United States

*** Corresponding Author:** Lili He,
Mailing Address: 240 Chenoweth Laboratory, 102 Holdsworth Way, Amherst, MA 01003,
E-mail: lilihe@foodsci.umass.edu,
Telephone: +1 (413) 545-5847

Inductively Coupled Plasma-Mass Spectrometry (ICP-MS). To determine the extraction efficiency of AgNPs from spinach leaves by organic solvent, AgNPs contaminated spinach leaves with organic solvent treatment were stored at ambient temperature prior to digestion. For the digestion process, spinach leaves were immersed with 3 mL HNO_3 (ACS reagent, 70%) in a 15 mL centrifuge tube overnight. Spinach leaves were microwaved to reach a temperature of 115 ℃ for 40 min, and then samples were cooled to room temperature. Five hundred µL of H_2O_2 was added to further digest the sample at 115 ℃ for 30 min. DI water was used to dilute the resultant digests to a total volume of 40 mL and then the diluent was filtered through polyethersulfone (PES) membrane prior to ICP-MS (Agilent 7500ce, Santa Clara, CA) analysis.

$$\eta_p = \left(\frac{[AgNPs]_{nominal} - [AgNPs]_{leaf}}{[AgNPs]_{nominal}}\right) \times 100$$

Where η_P refer to the extraction efficiency of AgNPs from plants.